A model to predict stream water temperature across the conterminous USA

HYDROLOGICAL PROCESSES
Hydrol. Process. **29**, 2178–2195 (2015)
Published online 14 October 2014 in Wiley Online Library
(wileyonlinelibrary.com) DOI: 10.1002/hyp.10357

A model to predict stream water temperature across the conterminous USA

Catalina Segura,[1,2]* Peter Caldwell,[3] Ge Sun,[4] Steve McNulty[4] and Yang Zhang[1]

[1] *Marine, Earth, and Atmospheric Sciences Department, North Carolina State University, 2800 Faucette Drive, Raleigh, NC 27695-8208, USA*
[2] *Forestry Engineering, Resources, and Management Department, Oregon State University, 280 Peavy Hall, Corvallis, OR 97331, USA*
[3] *Center for Forest Watershed Science, USDA Forest Service, Coweeta Hydrologic Lab 3160 Coweeta Lab Road, Otto, NC 28763, USA*
[4] *Eastern Forest Environmental Threat Assessment Center, USDA Forest Service, 920 Main Campus Drive, Venture Center II, Suite 300, Raleigh, NC 27606, USA*

Abstract:

Stream water temperature (t_s) is a critical water quality parameter for aquatic ecosystems. However, t_s records are sparse or nonexistent in many river systems. In this work, we present an empirical model to predict t_s at the site scale across the USA. The model, derived using data from 171 reference sites selected from the Geospatial Attributes of Gages for Evaluating Streamflow database, describes the linear relationship between monthly mean air temperature (t_a) and t_s. Multiple linear regression models are used to predict the slope (m) and intercept (b) of the t_a–t_s linear relation as a function of climatic, hydrologic and land cover characteristics. Model performance to predict t_s resulted in a mean Nash–Sutcliffe efficiency coefficient of 0.78 across all sites. Application of the model to predict t_s at additional 89 nonreference sites with a higher human alteration yielded a mean Nash–Sutcliffe value of 0.45. We also analysed seasonal thermal sensitivity (m) and found strong hysteresis in the t_a–t_s relation. Drainage area exerts a strong control on m in all seasons, whereas the cooling effect of groundwater was only evident for the spring and fall seasons. However, groundwater contributions are negatively related to mean t_s in all seasons. Finally, we found that elevation and mean basin slope are negatively related to mean t_s in all seasons, indicating that steep basins tend to stay cooler because of shorter residence times to gain heat from their surroundings. This model can potentially be used to predict climate change impacts on t_s across the USA. Copyright © 2014 John Wiley & Sons, Ltd.

KEY WORDS stream water temperature; water quality modelling; thermal sensitivity

Received 26 November 2013; Accepted 2 September 2014

INTRODUCTION

Stream water temperature is a key water quality parameter that impacts aquatic ecosystems (Whitehead *et al*., 2009). Water temperature controls the concentration of dissolved oxygen (Ozaki *et al*., 2003; Sand-Jensen and Pedersen, 2005) and the concentrations of pollutants (Ficke *et al*., 2007). Water temperature also affects biomass accrual and therefore habitat availability for many aquatic species (Beitinger *et al*., 2000; Ebersole *et al*., 2001; Danehy *et al*., 2005; Caissie, 2006; Webb *et al*., 2008; Mayer, 2012). Special concern has been raised about the likely response of water temperature to climate warming for cold water fish, such as salmon and trout, because their thermal habitat range is narrow in alpine locations with limited migration alternatives (Eaton and Scheller, 1996; Mohseni *et al*., 1999; Hari *et al*., 2006; Isaak *et al*., 2012).

Predicting stream temperature is challenging because it is controlled by many local and cumulative natural (e.g. meteorology, geology, hydrology and land cover) and anthropogenic (e.g. dams, water withdrawals and diversion and return flow from thermoelectric plants) factors. The energy balance of a river system is a function of the heat fluxes driven by solar radiation (Sinokrot and Stefan, 1993; Webb and Zhang, 1997; Boyd and Kasper, 2003), hydrologic inputs (Gu *et al*., 1998; Langan *et al*., 2001) and stream geomorphic structure (Poole and Berman, 2001). These local factors are affected by the existence or absence of shading from riparian vegetation (Brown and Krygier, 1970; Beschta, 1997; Roth *et al*., 2010; Studinski *et al*., 2012), channel geomorphology (Vannote *et al*., 1980; Hawkins *et al*., 1997; Poole and Berman, 2001; Webb *et al*., 2003; Johnson, 2004), hyporheic exchange (Evans and Petts, 1997), water discharge from industry, power plants and reservoirs (Edinger *et al*., 1968; Webb and Nobilis, 1994; Webb and Nobilis, 2007; Olden and Naiman, 2010; Poff *et al*., 2010) and water diversions (Meier *et al*., 2003). Cumulative stream temperature dynamics depends on upstream heat accumulation and groundwater inputs

*Correspondence to: Catalina Segura, Assistant Professor, Forestry Engineering, Resources, and Management Department, Oregon State University, 280 Peavy Hall, Corvallis, OR 97331, USA.
E-mail: catalina.segura@oregonstate.edu

(Kelleher *et al.*, 2012), which are influenced by land cover characteristics and urbanization (Nelson and Palmer, 2007).

Understanding and predicting changes in stream water temperature under climate change are of great interest to watershed managers and ecohydrologists. Several studies have highlighted evidence of stream water temperature increases over the last decades for many rivers across the globe (Stefan and Sinokrot, 1993; Pilgrim *et al.*, 1998; Morrill *et al.*, 2005; Ducharne, 2008; Kaushal *et al.*, 2010; Arismendi *et al.*, 2012; Wu *et al.*, 2012; van Vliet *et al.*, 2013). Some studies have analysed the historic record (Kaushal *et al.*, 2010; Arismendi *et al.*, 2012; Isaak *et al.*, 2012), whereas others have modelled future impacts using either process-based models (Norton and Bradford, 2009; Wu *et al.*, 2012; Ficklin *et al.*, 2013; van Vliet *et al.*, 2013) or statistically based models (Pilgrim *et al.*, 1998; Mohseni *et al.*, 2003; Morrill *et al.*, 2005; Mantua *et al.*, 2010) Early physically based models described temporal and spatial distributions of temperature within a water body by calculating heat exchange, on the basis of heat exchange through the evaporation process and conduction between the water body and the atmosphere (Edinger *et al.*, 1968; Brown, 1969). These models evolved to incorporate heat advection–dispersion transport equations (Haag and Luce, 2008; Yearsley, 2009) and net heat transfer processes at the water surface (Edinger *et al.*, 1968; Mohseni and Stefan, 1999; Bogan *et al.*, 2003). Many models explicitly couple a heat transfer to a process-based hydrologic model (Kim and Chapra, 1997; Younus *et al.*, 2000; Wu *et al.*, 2012; Loinaz *et al.*, 2013). Some physically based water temperature models have been explicitly linked to hydrologic models such as the Soil and Water Assessment Tool (Ficklin *et al.*, 2012), Hydrologic Simulation Program–FORTRAN (Bicknell, 1997; Chen *et al.*, 1998) and Variable Infiltration Capacity (van Vliet *et al.*, 2013). Even though great progress has been made using process-based models, their applications are limited because the hydrometeorological and watershed data inputs required to run these sophisticated models are lacking at many locations. Statistically or empirically derived models offer an alternative that requires significantly less data, which is especially challenging to acquire to represent the spatial variability in large areas (Eaton and Scheller, 1996; Mohseni *et al.*, 1999). Statistically based models are derived empirically from observations, attempting to describe the correlation between air and stream temperature using both linear (LM) and nonlinear models. The independent variables in these regressions include air temperature, discharge and lag time coefficients. These regression models have been derived at the hourly, daily, weekly and monthly scales using both linear and logistic functions (Table I). Some of these studies have highlighted that the strength of the fit between air and stream temperatures decreases with increasing temporal resolution for both LM and nonlinear model (Stefan and Preudhomme, 1993; Pilgrim *et al.*, 1998; Erickson and Stefan, 2000; Morrill *et al.*, 2005). Amongst the recent studies (Table I), some investigated regional sensitivity of stream temperature across different US regions including Pennsylvania (Kelleher *et al.*, 2012), the Pacific Northwest (Mayer, 2012) and the Southeast (Caldwell *et al.*, 2014). Recent studies have modelled the relationship between air and stream temperature from historical information to explore thermal sensitivity and potential climate change

Table I. Past studies that have investigated the relation between air (t_a) and stream temperature (t_s) during the last three decades

Model	Geographic location	Number of sites	Temporal scale	Reference
Linear	UK	6	5-day, weekly	Crisp and Howson (1982)
Linear	Mississippi, USA	11	Hourly, daily, weekly	Stefan and Preudhomme (1993)
Linear	UK	1	Monthly	Webb and Walling (1993)
Linear	Austria	1	Monthly	Webb and Nobilis (1994)
Linear	Oklahoma, USA	38	Daily, weekly, monthly	Erickson and Stefan (1996)
Linear	Austria	1	Monthly	Webb and Nobilis (1997)
Linear	Minnesota, USA	39	Daily, weekly, monthly	Pilgrim *et al.* (1998)
Logistic	USA	584	Weekly	Mohseni *et al.* (1998)
Linear/logistic	UK	4	Hourly, daily, weekly	Webb *et al.* (2003)
Linear	Japan	5/27	Daily/monthly	Ozaki *et al.* (2003)
Linear/logistic	Global	43	Daily, weekly	Morrill *et al.* (2005)
Linear	Pennsylvania, USA	12	Weekly	O'Driscoll and DeWalle (2006)
Linear	France	88	Monthly	Ducharne (2008)
Logistic	Pacific Northwest, USA	70	Weekly	Mantua *et al.* (2010)
Logistic	Global	157	Daily	van Vliet *et al.* (2011)
Linear/logistic	Pacific Northwest, USA	104	Weekly	Mayer (2012)
Linear/logistic	Pennsylvania, USA	57	Daily, weekly	Kelleher *et al.* (2012)
Linear/logistic	Southeast, USA	61	Monthly	Caldwell *et al.* (2014)
Linear/logistic	France	1	Daily	Bustillo *et al.* (2014)

impacts. Thermal sensitivity (i.e. the slope of the linear relation between air and stream temperature) correlates with stream size and groundwater influence (Ozaki *et al*., 2003; O'Driscoll and DeWalle, 2006; Ducharne, 2008; Kelleher *et al*., 2012; Mayer, 2012).

Although several studies have used a statistical approach to model stream temperature (Table I), no regional-to-continental scale statistically based models capable of predicting stream temperature in the absence of historical temperature data have yet been formulated. In addition, no study has systematically investigated seasonal watershed controls on water temperature except for an analysis of the summer for sites in the Pacific Northwest (Mayer, 2012). The objectives of this investigation are the following: (1) to formulate a model to predict the relation between mean monthly air (t_a) and stream water (t_s) temperatures across the conterminous US (CONUS) and (2) to investigate watershed controls over seasonal thermal sensitivity and mean seasonal t_s at the CONUS.

METHODS

Study area and datasets available

We considered 1947 reference sites across the CONUS identified in the Geospatial Attributes of Gages for Evaluating Streamflow, version II (GAGES II) (Falcone *et al*., 2010; Falcone, 2011). All these sites had at least 20 years of discharge records since 1950 or were active as of water year 2009. Reference streamflow gauges were selected from the least disturbed watersheds on the basis of indicators such as hydrologic disturbance index, pertinent annual data report, remarks regarding flow alteration and screening comments from NAWQA personnel visual evaluation (Falcone *et al*., 2010; Falcone, 2011). We acquired the daily stream water temperature databases available from the U.S. Geological Survey National Water Information System website for all of these 1947 sites.

For the analysis at the monthly resolution, we included sites with at least 20 months of stream water temperature data between 1960 and 2012 derived from at least 20 daily mean observations for each month. For the weekly (i.e. 7-day mean) analysis, we included sites with at least 40 data pairs (t_a–t_s) derived from complete 7-day mean series between 1980 and 2012. The minimum number of observations to consider was determined on the basis of the analysis of several sites with long periods in record (>180 months or 300 weeks) as follows. We fitted a linear function between t_a and t_s for subsets of data from these sites with 5–180 months for the monthly time series and with 5–300 weeks for the weekly data. We computed the best fitted slope and R^2 of the linear fits between t_a and t_s for each subset. Subsequently, we compared these parameters (m and R^2) to the m and R^2 computed when the complete dataset was included (Figure 1). We found that a minimum sample size of around 20 observations for monthly data and 40 observations for weekly data was sufficient as the difference between slopes and R^2

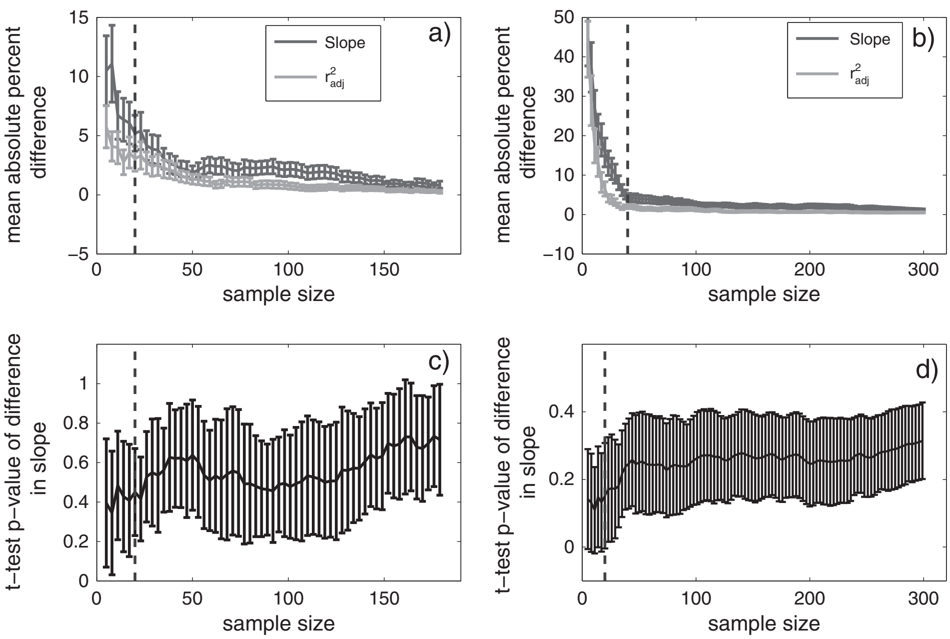

Figure 1. Mean absolute difference between the best fitted slope (m) and adjusted R^2 of the linear relation between t_a and t_s and fitted m and R^2 with varying samples sizes for 19 sites at the monthly time scale (panel a) and 32 sites at the weekly time scale (panel b). p-value of the difference between best fitted m considering all data available and best fitted m considering subsets of data for monthly (panel c) and weekly (panel d) data

decreases significantly at approximately 20 or more observations (Figure 1).

Considering the aforementioned criterion of 20 and 40 data pairs, we found 176 and 185 out of the 1947 reference sites in the GAGES data base suitable for monthly and 7-day analyses, respectively. Five sites located in Wyoming (WY) were discarded because they were strongly influenced by Yellowstone geothermal features. Therefore, the total dataset considered included 171 sites for monthly analyses and 180 sites for 7-day mean analyses. These sites are located in 32 states and 16 of the 18 hydrologic regions of the country (Figure 2). A second group of 95 sites with monthly data was used to test the applicability of a model derived on the basis of reference sites anywhere in the CONUS. These sites were extracted from the 1176 nonreference sites identified in GAGES II with a disturbance metric less than 10. This disturbance score corresponds to the 25 percentile of all 9068 nonreference sites. In general, these sites are characterized by low dam density (<1.4 dams per 100 km^2), low road density (<3 km/km^2) and low level of channelization (<3% coded as 'canal', 'ditch' or 'pipeline' in NHDPlus, http://nhd.usgs.gov/index.html). We found 139 sites out of 1176 having stream temperature data but only 99 having at least 20 months of both stream and water temperature data (Figure 2) and 89 considering $t_a > 0\,°C$. The range of drainage areas amongst the sites considered (reference and nonreference) is 2–14 000 km^2 with elevation varying between 2 and 3000 m (Figure 2). Historic monthly air temperature data (t_a) were acquired from the 4 km × 4 km gridded data generated by the PRISM Climate Group (http://www.prismclimate.org) for all reference and nonreference sites (Figure 2). Daily historic gridded 1 km × 1 km data from

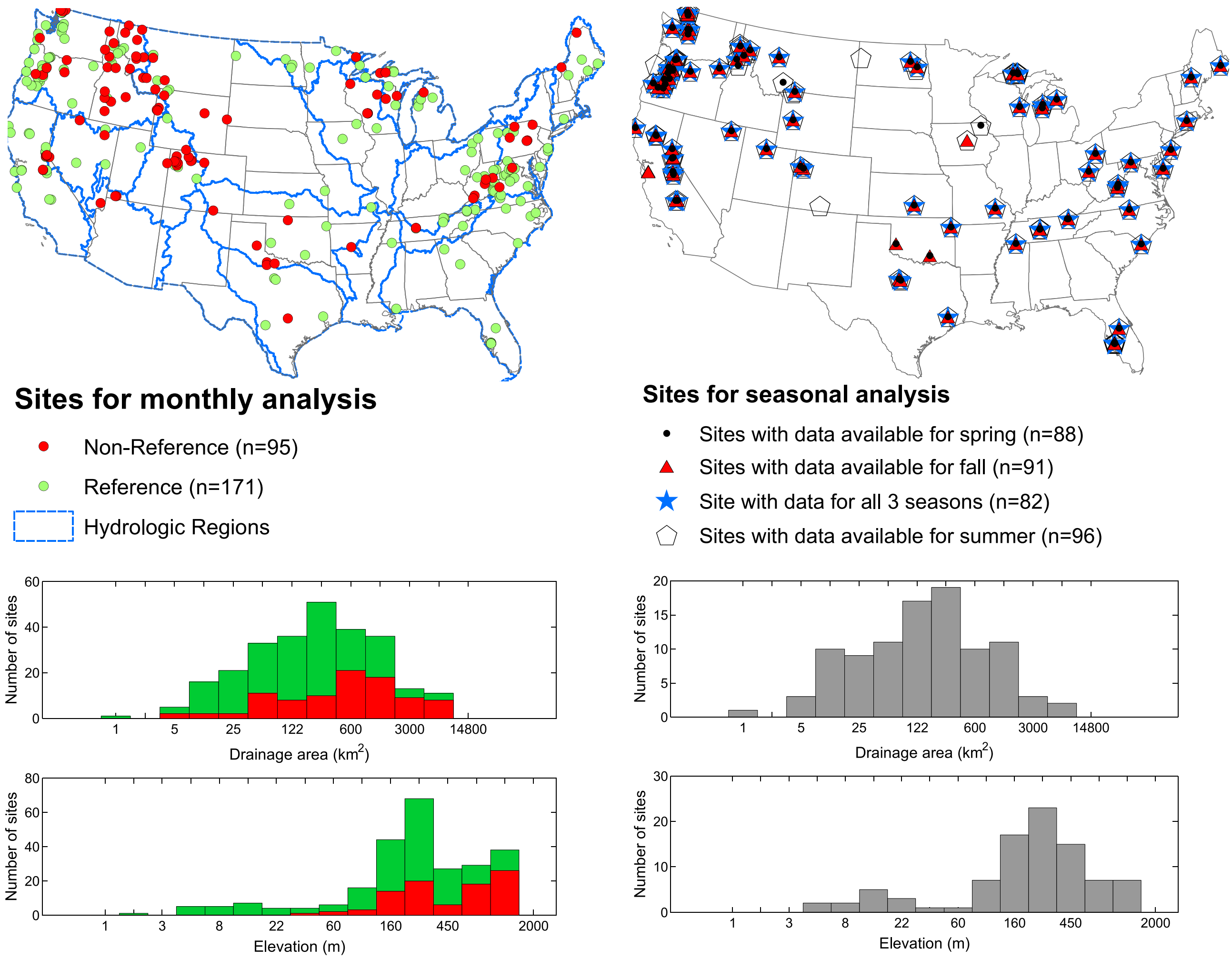

Figure 2. Location and characteristics of sites considered for monthly (left) and seasonal analyses (right). Bottom histograms present the distributions of drainage area and elevation. Reference sites are depicted in green ($n = 171$) and nonreference sites are depicted in red ($n = 95$). The histograms in the right correspond to those sites considered for the summer season analysis ($n = 96$)

the Daily Surface Weather and Climatological Summaries, Daymet (Thornton *et al*., 2012) were obtained for all reference sites to develop 7-day mean values.

Relationship between monthly mean air and stream water temperature

The relationship between mean monthly t_a and t_s at each reference site was characterized by considering two different models: (1) an LM based on t_a and (2) a three-parameter logistic function (LOM). The LM describes mean monthly t_s values as a linear function of mean monthly t_a, considering all observations and also excluding data pairs with t_a less than 0 °C (refer to the succeeding texts). The model parameters include the slope (m) of the line and the intercept with the y-axis (b). The use of this type of model dates back to the 1980s, and it has been used to describe stream water temperature in Pennsylvania (O'Driscoll and DeWalle, 2006; Kelleher *et al*., 2012), Minnesota (Pilgrim *et al*., 1998), Mississippi (Stefan and Preudhomme, 1993), Oklahoma (Erickson and Stefan, 2000) and some European locations (Crisp and Howson, 1982; Webb and Walling, 1993; Webb and Nobilis, 1994; Webb and Nobilis, 1997; Webb *et al*., 2003; Ducharne, 2008). The advantage of this model is that it is simple requiring only two parameters (i.e. m and b in Table II).

The three-parameter LOM was originally formulated with four parameters (Mohseni, *et al*., 1998) and describes the t_a–t_s relation with an 's-shape' function defined by a minimum temperature (μ), a maximum temperature (α), an inflection characterized by a temperature (β) and a slope (γ). We used a three-parameter version of this model by setting the minimum temperature μ to 0 °C (Caldwell *et al*., 2014). The LOM has been widely used in many studies since 1998 (Table I). This model has been found to be superior to the LM to describe mean weekly t_s data (e.g. Mohseni and Stefan, 1999; Webb *et al*., 2003; Mayer, 2012). However, the LM has proven to be a reliable alternative to the LOM when describing the t_a–t_s relation at the monthly time step in many locations. For example, Ducharne (2008) and Caldwell *et al*. (2014) found that an LM was adequate to describe monthly stream water temperature at 88 French sites and 61 sites located in the southeastern region of the USA, respectively. The advantage of the LOM over the LM appears to be evident for air temperature below 0 °C regardless of the data resolution (Mohseni *et al*., 1998; Morrill *et al*., 2005; Kelleher, *et al*., 2012) because of the nonlinear behaviour observed below subfreezing air temperatures. The LOM has been found to be superior to the LM for modelling weekly, daily and hourly temporal resolutions over the whole range of observed t_s (Mohseni and Stefan, 1999; Webb, *et al*., 2003; Morrill, *et al*., 2005; Mantua, *et al*., 2010; van Vliet, *et al*., 2011). However, no study has accessed the relative advantage of the LOM over the LM at the monthly time scale except for Caldwell *et al*. (2014) who found no statistical advantage of LOM over the LM.

For both models, the best parameter sets were determined using least squares statistics (LM) or by minimizing the sum of the square differences between model and observations (LOM). The range of parameter values tested for each parameter of the LOM was set to be sufficiently wide to allow an unconstrained identification of best parameter values ($\mu = 0$ °C, $\alpha = 1$–55 °C, $\beta = 1$–30 °C and $\gamma = 0$–90°). Best parameters were estimated for each site in MATLAB (MATLAB, 2010) by simultaneously varying parameter sets over a uniform grid of more than 1 000 000 values and finding the parameter set that yields the lowest overall sum of the squared differences between the observed and calculated mean monthly t_s.

Table II. Functions considered for modelling the relation between air (t_a) and stream water (t_s) temperature at each site and number of sites considered in the monthly and weekly analysis

			Number of sites considered (Figure 1)	
Model	Equation	Parameters of the model	Monthly analysis[a]	Weekly analysis for $t_a > 0$°°C[b]
Linear: LM	$t_s = mt_a + b$	m: slope b: intercept	Complete series ($n = 171$) [b] Series with $t_a > 0$ °C ($n = 158$)	Spring ($n = 88$) Summer ($n = 96$) Fall ($n = 91$)
Logistic: LOM	$t_s = \mu + \frac{\alpha - \mu}{1 + \exp(\gamma(\beta - t_a)}$	μ: minimum t_s set to zero α: maximum t_s β: temperature at inflection γ: maximum slope of the relation between t_a and t_s	Complete series ($n = 171$)	

[a] With at least 20 observations per site.
[b] With at least 40 observations per site.

Statistical methods to formulate a regional model

Ordinary least squares regression methods in MATLAB were used to obtain a regional model to predict the parameters (e.g. m and b in the LM) that best describe the relations between t_a and t_s, considering all reference sites simultaneously:

$$y_n = X_1\beta_1 + X_2\beta_2 + X_3\beta_3 + \ldots + X_n\beta_{1n} + \beta_0 \quad (1)$$

where y_n are the parameters of the LM (m or b), X_1 through X_n are basin characteristics and β_o through β_n are model coefficients. A similar approach has taken by Ducharne (2008) who attempted to predict linear parameters of the t_a–t_s relation using stream order as a predictor variable. Here, we considered 17 basin characteristics as potential predictors of the values of m and b. These data were acquired from the GAGES II database (Table III) and were selected to represent different factors that could potentially influence the thermal regime of a river system. Previous studies have highlighted the importance of channel size and topography (e.g. Beschta and Weatherred, 1984; Ducharne, 2008); therefore, we consider drainage area (*DA*), elevation (*H*) and mean basin slope (*S*) as potential predictors. The importance of groundwater and subsurface and overland contributions to the thermal regime have been discussed by others (Bicknell, 1997; Chen *et al.*, 1998; Younus *et al.*, 2000; Story *et al.*, 2003; O'Driscoll and DeWalle, 2006; Tague *et al.*, 2007); thus, in this study, we included available hydrologic variables related to total discharge (mean annual runoff, *Q*) and groundwater contribution and the relative proportion of different runoff generation mechanisms [base flow index (*BF*), Dunne overland flow (*DOF*), Horton overland flow (*HOF*), topographic wetness index (*TWI*) and subsurface flow contact time (*C*)]. The importance of climatic and atmospheric factors (e.g. Sinokrot and Stefan, 1993) was also considered by including mean annual precipitation, *P*, mean annual temperature, *T*, and watershed aspect, *AS*, as potential predictors. Finally, we also

Table III. Independent variables considered in multiple linear regression models (Falcone *et al.*, 2010; Falcone, 2011)

Variable	Description	Extent	Unit
DA	Watershed drainage area	Watershed	km^2
P	Annual mean precipitation in the basin (1971–2000)	Watershed	cm
T	Annual mean air temperature at the gauge locations (1971–2000)	Site	°C
BF	Base flow index: ratio of base flow to total streamflow, expressed as a percentage and ranging from 0 to 100. Base flow is the sustained, slowly varying component of streamflow, usually attributed to groundwater discharge to a stream (Wolock, 2003)	Watershed	%
DOF	Dunne overland flow, also known as saturation overland flow, is generated in a basin when the water table 'outcrops' on the land surface (because of the infiltration and redistribution of soil moisture within the basin), thereby producing temporary saturated areas. These saturated areas generate Dunne overland flow through exfiltration of shallow groundwater and by routing precipitation directly to the stream network. The data are estimated from a watershed simulation model – TOPMODEL (Wolock, 1993). The model was run throughout the conterminous USA	Watershed	%
HOF	Horton overland flow, also known as infiltration excess overland flow, is generated in a basin when infiltration rates are exceeded by precipitation rates. The data are estimated from a watershed simulation model – TOPMODEL (Wolock, 1993). The model was run throughout the conterminous USA	Watershed	%
TWI	Topographic wetness index, ln(a/S); where 'ln' is the natural log, 'a' is the upslope area per unit contour length and 'S' is the slope at that point. See http://ks.water.usgs.gov/Kansas/pubs/reports/wrir.99-4242.html and Wolock and McCabe, 1995 for more details	Watershed	Ln (m)
C	Subsurface flow contact time index. The subsurface contact time index estimates the number of days that infiltrated water resides in the saturated subsurface zone of the basin before discharging into the stream (Wolock *et al.*, 1989; Wolock, 1997)	Watershed	Days
Q	Estimated watershed annual runoff, mm/year, mean for the period 1971–2000 (Krug *et al.*, 1989)	Watershed	mm/year
U	Watershed percentage 'developed' (urban), 2006 [sum of low, medium and high intensity development and open space in the watershed (classes 21–24)]	Watershed	%
F	Watershed percentage 'forest', 2006 [sum of deciduous forest, evergreen forest and mixed forest (classes 41, 42 and 43)]	Watershed	%
*U*1	Mainstem 100 m buffer 'developed' (urban), 2006 [sum of low, medium and high intensity development and open space in the watershed (classes 21–24 in a buffer 100 m each side of stream centerline)]	RIPARIAN 100 m	%
*F*1	Mainstem 100 m buffer 'forest', 2006 [sum of deciduous forest, evergreen forest and mixed forest (classes 41, 42 and 43 a buffer 100 m each side of stream centerline)]	RIPARIAN 100 m	%
H	Elevation at gauge locations	Site	m
S	Mean watershed slope	Watershed	%
AS	Mean watershed aspect, degrees (degrees of the compass, 0–360)	Watershed	°

considered the importance of shading to the stream from the riparian area and the influence of land cover type (LeBlanc *et al*., 1997; Moore *et al*., 2005; Allen *et al*., 2007; Richardson and Danehy, 2007; Booth *et al*., 2014) by including the percent urban (*UR*, *UR1*) and forested (*F*, *F1*) in the basin and riparian area of the main channel in the analysis (Table III). The full description of these variables can be obtained from the original sources (Falcone *et al*., 2010; Falcone, 2011).

We used stepwise linear regression to find the best models, considering 17 independent variables (Table III). The models were selected to maximize the predictive power (R^2). A variable was kept in the final model if it significantly improved its predicting power ($p < 0.05$). The number of variables in each model was limited to a maximum of six to avoid over parameterization. This approach was also taken by others using a similar set of independent variables (Roman *et al*., 2012). Multicolinearity was assessed by computing the variance inflation factor (VIF) (Marquard, 1970). A VIF greater than ten was considered indicative of a serious multicolinearity problem. We assessed the distribution of residuals to ensure their independence and normal distribution by visual inspection of histograms and Normal Q-Q plots (i.e. plot of the residual quantiles *vs* theoretical quantiles from a normal distribution) together with the normality test proposed by Shapiro–Wilk test (Shapiro and Wilk, 1965). This test evaluated the null hypothesis that a sample (in or case the residuals of the regression model) came from a normally distributed population.

Seasonal thermal sensitivity

The slope, *m*, of the linear relation between t_a and t_s is often interpreted as a measure of thermal sensitivity (Kelleher *et al*., 2012; Mayer, 2012). We computed this parameter for the spring, summer and fall seasons independently, on the basis of weekly temperature data. The historical time series were built on the basis of 7-day mean values derived from the U.S. Geological Survey stream water temperature daily data and from daily air temperature data from the Daymet data (Thornton *et al*., 2012). We decided to use 7-day mean values rather than monthly data because the time series from the monthly series per season would in many cases include less than five t_a–t_s pairs. In addition, 7-day mean data captures more variability whilst still providing strong statistical information regarding the linear relation (Stefan and Preudhomme, 1993; Erickson and Stefan, 1996; Pilgrim, *et al*., 1998; Kelleher, *et al*., 2012). Spring was defined as weeks 10–22 of a calendar year (5 March to 14 June), summer between weeks 23–35 (5 June to 1 September) and fall defined as between weeks 36 and 48 (2 September to 1 December). We investigated the relationships between thermal sensitivity and basin characteristics (Table III) for each season to establish the existence of temporal basin controls. In addition, we evaluated the controls of drainage area, precipitation, discharge, base flow index, forest cover, elevation and mean basin slope, on spring, summer and fall mean t_s temperatures. We considered the use of the weekly data to develop the regional model to predict the linear relation between air and stream temperature; however, we found that the predicting power was weaker than using the monthly data, and therefore, we only present monthly data here.

RESULTS AND DISCUSSION

Relationships between monthly air and stream water temperatures

Figure 3 presents examples of the LM and LOM fits at five sites across the CONUS including monthly (t_a, t_s) pairs over the complete range of temperature observations. The R^2 values in these five cases were greater than 0.93 for all models. These sites are representative examples of the results in all basins considered. The range of best fitted parameters for the LOM and LM is summarized in Table IV. The parameters of the logistic fit

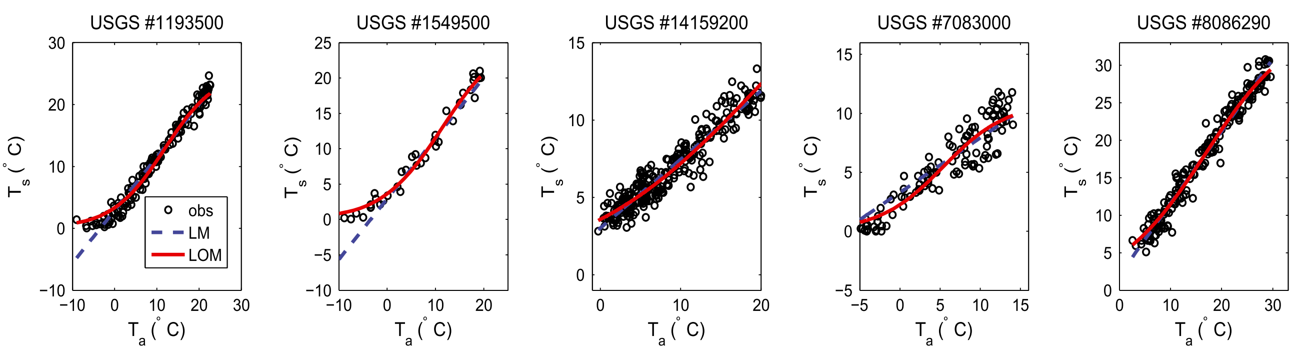

Figure 3. Examples of the linear model (LM) and logistic operating model (LOM) fits to describe the relation between air (t_a) and stream (t_s) temperatures at five U.S. Geological Survey (USGS) sites: #01193500 (Salmon River near East Hampton, CT), #01549500 (Blockhouse Creek near English Center, PA), #14159200 (SO FK McKenzie River Abv Cougar Lake near Rainbow, OR), # 07083000 (Halfmoon Creek near Malta, CO) and # 08086290 (Big Sandy Creek, TX)

Table IV. Mean and standard deviation of coefficient of determination (R^2) and best fitted parameter ranges for the linear (LM) and logistic model (LOM) to monthly time series

Variable	LM ($n = 171$)	LOM ($n = 171$)	LM ($n = 158$), $t_a > 0°°C$
R^2	0.94 ± 0.05	0.96 ± 0.04	0.94 ± 0.06
Slope, m	0.76 ± 0.18	—	0.8 ± 0.19
Intercept, b	2.5 ± 1.7	—	1.88 ± 1.6
α	—	30.2 ± 10.2	—
β	—	15.8 ± 5.6	—
γ	—	0.15 ± 0.05	—

were within the tested range at 165 sites (96%). The best fitted values of α (maximum monthly temperature) for five sites were equal to the upper tested value (51 °C). Further increment of the tested range indicated that the stream water temperatures at these sites had no tendency to become constant in the upper range. Similarly, the best fitted β (temperature in the inflection point) for one site was equal to the upper tested value of 30 °C, indicating that the data did not have an inflection.

The mean R^2 by all models was greater than 0.94 (Table V; Figure 4). The mean R^2 for the LM fits was significantly smaller than the R^2 of the LOM ($p < 0.0001$). The LOM fits were superior to the LM at 132 sites (77% of the total sites used). The differences between R^2 values were up to 25% (Figure 4). However, at most sites (90%), the difference between R^2 values was less than 4.5%. The sites with differences greater than 4.5% were characterized by having a significant number of t_a observations less than 0 °C (20–52% of the observations). These 16 sites are located at latitudes above 41°N in Iowa (IA), Maine (ME), Michigan (MI), Minnesota (MN), Montana (MT), North Dakota (ND), Pennsylvania (PA), Wisconsin (WI) and Wyoming (WY). The locations of these 16 sites highlight the advantage of the LOM to describe the relationship at temperatures less than 0 °C. The difference between adjusted R^2 by the LM and the LOM was nonsignificant ($p > 0.05$) excluding the aforementioned 16 sites. Furthermore, there was no significant difference in the fit between the LM and the LOM, considering $t_a > 0$ °C ($p = 0.46$). Given the fact that no statistical advantage was found for the LOM model over the LM for air temperatures greater than 0 °C, we decided to select the model with fewer parameters (i.e. LM) and focused only on $t_a > 0$ °C. Under this consideration, our sample size decreased from 171 to 158 sites, each with at least a total 20 months of temperature data. The slope of the

Table V. Percentage of the variance explained by the independent variable considered in predicting models for (A) the parameters of the linear model (LM) (slope, m and intercept, b, Equations (2)–(5)), (B) the seasonal thermal sensitivity (m) and (C) the mean seasonal stream temperature (t_s)

Sample	LM variable	n	R^{2a}	DA^b	P	T	Q	BF	HOF	C	F	$F1$	$U1$	H^b	S
(A) Variables considered in predicting m and b of the LM															
All sites	m	158	0.54	25.3	2.4			19.3				3.3		4.8	
All sites	b	158	0.14	4.9					3.0			7.4			
$H > 970$ m	b	23	0.47				50.0								
200 m < H < 970 m	b	90	0.25	6.5					9.2	4.5	7.8				
$H < 200$ m	b	45	0.47	10.4		13.7			6.4			14.4	8.3		
(B) Variables considered in predicting seasonal thermal sensitivity (m)															
Spring	m	88	0.60	3.2				4.8							53.6
Summer	m	96	0.17	13.7			4.8								
Fall	m	92	0.45	17.1	4.1			21.5						4.4	
(C) Variables considered on predicting mean stream temperature (t_s) for three seasons (variables with – where omitted in the models)															
Spring	t_s	180	0.92	2.0		73.6	1.3	1.2	—	—		0.2	—	0.5	13.1
Summer	t_s	180	0.89	7.2		22.3	1.3	3.9	—	—	0.6		—	0.6	53.6
Fall	t_s	180	0.85	2.2		77.6		0.7	—	—		0.5	—		4.7
Spring	t_s	180	0.73	0.8	0.7	—	11.2	43.2	—	—			—	17.6	
Summer	t_s	180	0.82	5.9		—	3.4	16.0	—	—			—	3.6	53.6
Fall	t_s	180	0.63	0.9	1.4	—	5.3	18.0	—	—			—	38.3	

All variables explain a significant portion of the variance ($p < 0.05$).
Shaded cells indicate a positive relation.
Refer to Table III for variables descriptions.
[a] Adjusted R^2.
[b] Natural log transformed.

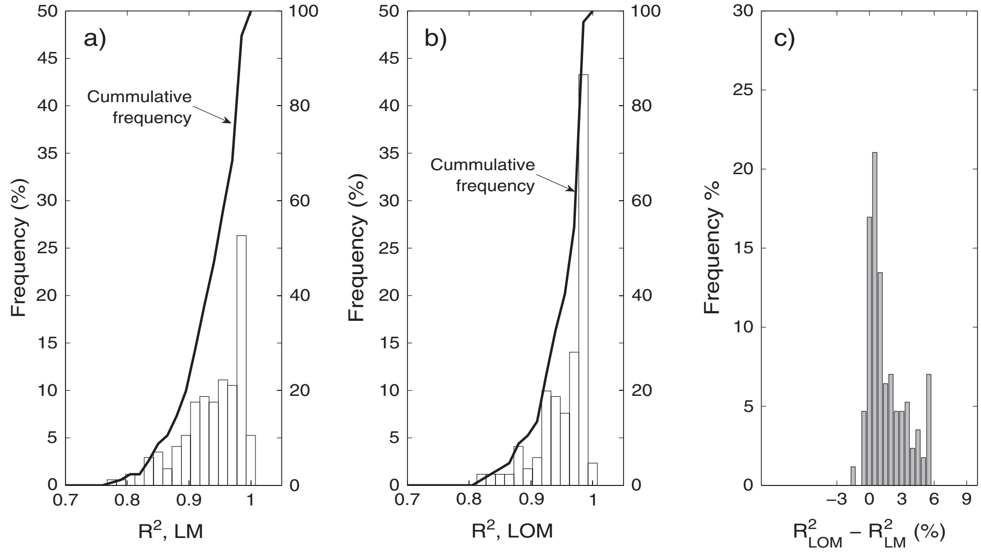

Figure 4. R^2 distributions of the linear (LM) and logistic (LOM) fits to the t_a–t_s relation at 171 sites (panels a and b) and distribution of the difference between the R^2 yield by the two functions (panel c)

LM (m) for these sites varied between 0.13 and 1.25 with a mean value of 0.8. The range of intercepts (b) values varied between −4 and 8 °C with a mean of 1.9 (Table IV and Figure 5). The range of m values was similar to those reported for sites in Oklahoma with a mean of 0.89 (Erickson and Stefan, 1996), Minnesota with a mean of 1.04 (Pilgrim *et al.*, 1998) and the Krems River in Austria with a mean of 0.69 (Webb and Nobilis, 1997). No clear spatial pattern in the distributions of m and b was found (Figure 5). However, there was a strong inverse correlation between them ($R^2 = 0.35$, $p < 0.00001$). This relation has also been observed by others (O'Driscoll and DeWalle, 2006; Ducharne, 2008) and indicates that stream water temperature tends to increase faster with increasing air temperature in sites with the lower intercept. This could be an expression of the buffering effect of groundwater contributions that may decrease the rates of t_s change with t_a (i.e. lower slope). More details on this topic are discussed in the succeeding texts.

Regional model to estimate m and b parameters

We considered hydrologic, land cover and physiographic variables as potential predictors of the slope (m) and intercept (b) of the LM between t_a and t_s (Table III). Simple models using only one predictor variable were insufficient to describe the observed variability in the values of m and b. R^2 values of the simple relations between variables in Table III and m and b were between 0.04 and 0.25. Therefore, we used stepwise multiple linear regressions to find stronger models, considering multiple independent variables simultaneously. Our analysis indicated that 5 out of the 17 variables considered explained a statistically significant ($R^2 = 0.54$, $p < 0.05$) portion of the variance in m:

$$m = 0.055\ln(DA) - 0.004BF - 0.047\ln(H) - 0.001(P) + 0.002F1 + 0.993 \quad (2)$$

where DA is drainage area, BF is base flow index, H is the elevation at the site, P is mean annual basin precipitation and $F1$ is forested cover in the 100 m buffer from the main channel (Figure 6). The mean percent difference between observed and modelled slope (m) was less than 10% at 93 sites (59%) and less than 25% at 134 sites (85%). The distribution of residuals is random, independent and reasonably close to a normal distribution as confirmed by visual inspection (i.e. histograms and probability plots) (Figure 6) and according to the Shapiro–Wilk test ($p > 0.05$). In addition, none of the variables included in the model had indication of multicolineary issues (VIF scores were all less than 3).

Drainage area and BF together explained 45% of the m variance (Table V). The relationship between m and DA was positive, indicating that larger catchments tend to have steeper relations (i.e. higher m). A positive relationship between basin size (either drainage area or stream order) and m was also reported in other studies such as 57 streams in Pennsylvania (Kelleher *et al.*, 2012), 183 sites in Idaho (Donato, 2002) and 88 sites in France (Ducharne, 2008). Kelleher *et al.* (2012) argued that the positive relation is the result of higher heat accumulation through the stream network for large basins. Whereas Ducharne (2008) believes that the dependence observed between stream order and the m and b results from the convergence of water temperature towards

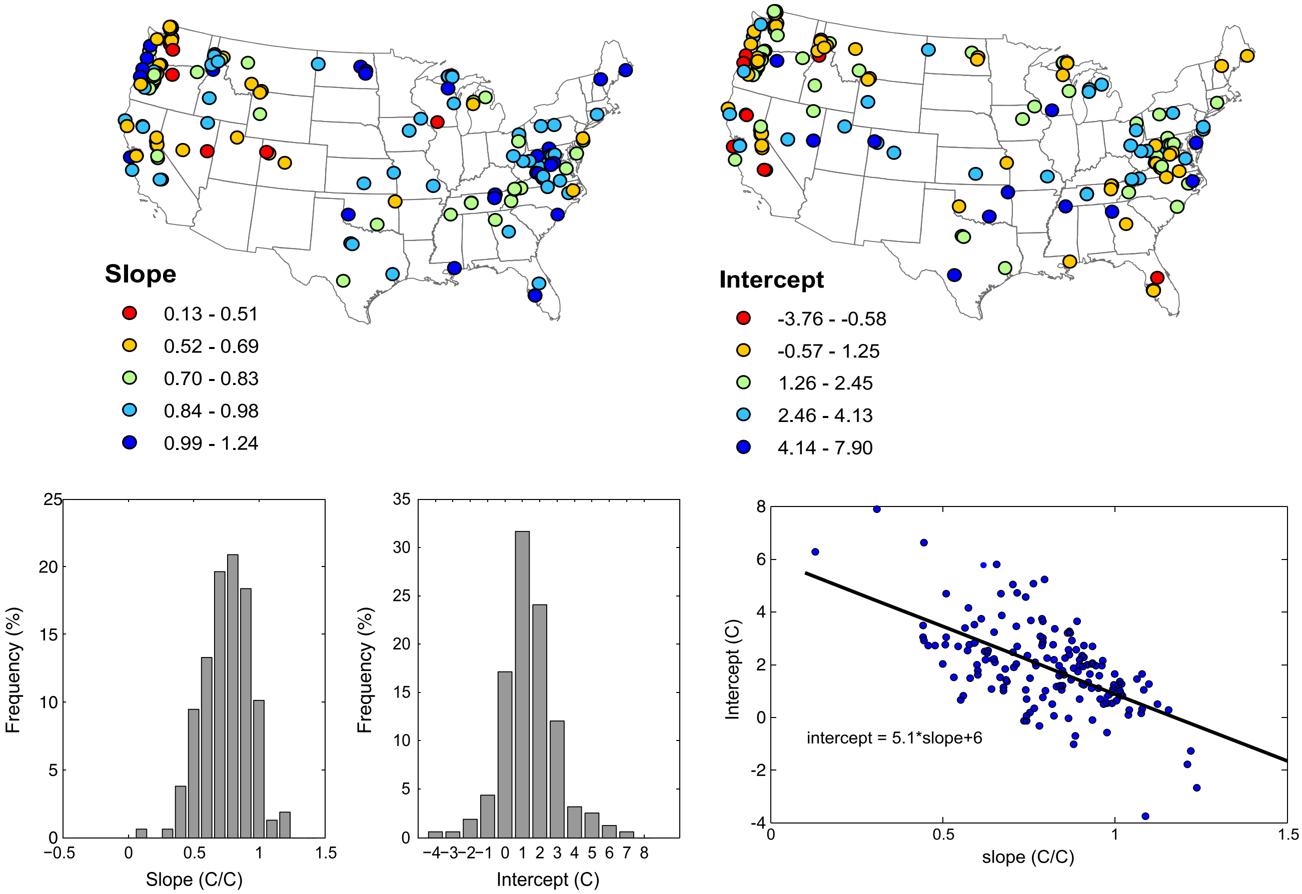

Figure 5. Spatial distribution of the parameters of the linear model (LM) between monthly t_a and t_s at 158 reference sites

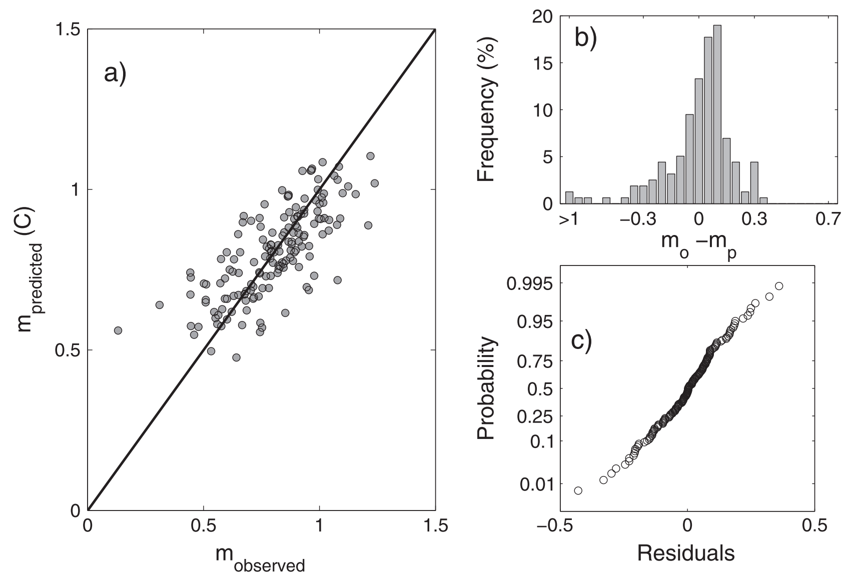

Figure 6. (Panel a) Observed and predicted slope (m), (panel b) distribution of the difference between observed and predicted m and (panel c) probability plot of the residuals at 158 reference sites

equilibrium temperature as water flows downstream. The relevance of *DA* as predictor of hydrologic behaviour is well recognized at multiple scales (Gupta *et al*., 1994; Vogel and Sankarasubramanian, 2000; Furey and Gupta, 2005; Segura and Pitlick, 2010; Segura *et al*., 2012; Segura *et al*., 2013). Further process-based research is lacking to understand the mechanistic relations between t_s nd *DA*. The relationship between *m* with *BF* was negative and indicated that as the proportion of groundwater influence increases, the slope of the relation between t_a and t_s decreases. This is probably an expression of the cooling effect of groundwater during summer by groundwater influx. This buffering effect of groundwater on stream temperature has also been reported by others (Erickson and Stefan, 2000; Younus *et al*., 2000; Story *et al*., 2003; O'Driscoll and DeWalle, 2006; Tague *et al*., 2007; Kelleher *et al*., 2012; Mayer, 2012). Elevation (*H*), precipitation (*P*) and forested cover in the riparian area (*F1*) each explained less than 5% of *m* variance (Table V) but were still significant ($p < 0.05$).

A model to predict the intercept (*b*) of the LM including all sites simultaneously yielded a poor performance ($R^2 = 0.14$, $p = 0.01$). The independent variables of this model are *F1* that explained 7.4% of the variance, *DA* that explained 4.8% and Horton overland flow (*HOF*) that explained 3% of the intercept variance (Table V). The relationships between *b* and *F1* and *b* and *DA* are both negative, indicating that *b* tends to decrease with increasing basin size and percent forest cover. This last relation is an expression of the cooling effect of shading from riparian vegetation. A significant negative relation between stream size and *b* has also been reported for other sites (Ducharne, 2008).

Given that the model to predict *b* including all sites was weak, we investigated alternative models by considering three altitude ranges ($R^2 = 0.25$–0.47, $p = 0.001$–0.006, Figure 7 and Table V):

$$H > 970m: \qquad b = -0.006Q + 3.85 \tag{3}$$

$$200m < H < 970m \qquad b = -0.27\ln(DA) + 0.08HOF + 0.003C + 0.02F + 5.05 \tag{4}$$

$$H < 200m \qquad b = -0.62\ln(DA) - 0.24T + 0.15HOF - 0.06U1 + 0.04F1 + 9.8 \tag{5}$$

where *Q* is the mean annual discharge, *C* is the contact time, *F* is the percentage forest cover in the basin and *T* is the annual mean air temperature at the site. The absolute errors for the intercept were less than 1 °C for 63% of the sites and less than 2 °C for 90% of the sites. As in the case of the model for the slope, the distribution of residuals in the intercept model is random, independent and normally distributed (Figure 7). The Shapiro–Wilk test yielded *p*-values >0.05. In addition, none of the variables included in the model had VIF scores greater than 3, indicating no multicollinearly issues in the final models.

For catchments greater than 970 m in elevation, a simple regression model based on *Q* was sufficient (Equation (3)). According to the model, *b* decreases as discharge increases. This is probably a reflection of increasing heat capacity with increasing discharge and decreased residence time reported by others (Webb *et al*., 2008; Mayer, 2012).

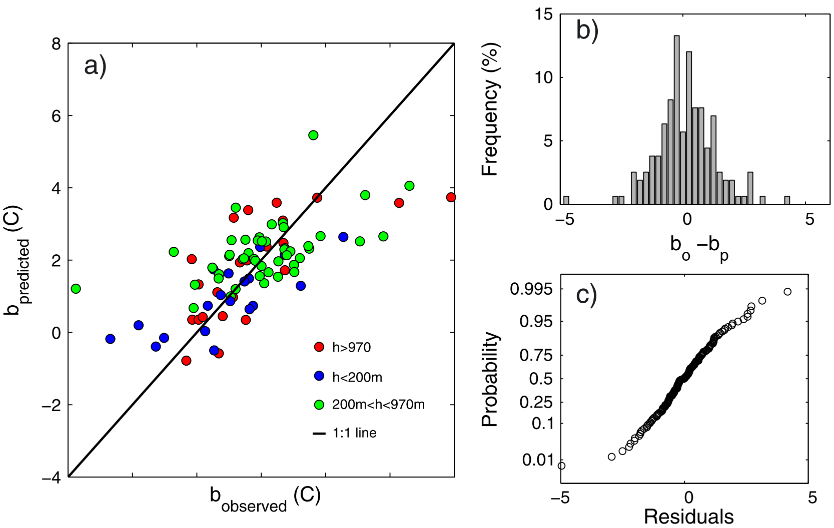

Figure 7. (Panel a) Observed and predicted intercept (*b*), (panel b) distribution of the difference between observed and predicted *b* and (panel c) probability plot of the residuals at 158 reference sites

For catchments between 200 and 970 m in elevation, the predicting model for b has four dependent variables. Percent Horton overland flow (*HOF*) explained the largest proportion of the intercept variance (9%). The *b-HOF* relation was positive, likely an expression of cooler water temperatures from water delivered to streams over surface flow paths as supposed to warmer water temperatures delivered via groundwater flow. This would be particularly true during the winter months because groundwater inputs to streams can be significantly warmer than surface water. However, this interpretation would not apply for the summer months in which groundwater could provide cooler water sources to streams. In the absence of seasonal estimates of *HOF*, it is not feasible to investigate this issue further. Percentage of forest in the basin (F) explained 8% of the intercept variance. This relation indicated that the location of the t_a–t_s relation with respect to the y-axis decreased with increasing forest cover (i.e. the shading effect). Drainage area explained 7% of the variance. This relation is negative and indicates that small basins tend to have larger intercepts, probably because a larger proportion of the stream flow is influenced by groundwater as opposed to water inputs from upstream. This was partially confirmed by the negative correlation between b and contact time (C), which explained 5% of the intercept variance.

The model derived to predict the intercept at sites less than 200 m had five variables. Forest cover in the riparian area (*F1*) was the strongest dependent variable in this model, explaining 14.4% of the variance. This relationship was negative, indicating that the higher the percent forest cover in the riparian area, the lower the intercept in the t_a–t_s relation (i.e. shading effect). Mean annual air temperature (T) also explained a significant proportion of the intercept variance (13.7%). The *T-b* relation was negative, indicating that the lower the annual mean air temperature, the higher the intercept of the relation. This relationship could be explained by the fact that T and H were inversely correlated ($R^2 = 0.33$ $p < 0.00001$). As in the case for sites located between 200 and 970 m in elevation, b decreased with increased *DA*, which explained 10.4% of the intercept variance. The percent of urban cover in the riparian area explained 8% of the variance and indicated a negative relation. We interpreted this in light of the positive relation between *HOF* and b. We argue that as the percentage of area with limited infiltration capacity increases in the riparian area, the temperature in the stream decreases because of the associated increase in surface dominated runoff (i.e. *HOF*), which introduces cooler water to streams than does the base flow condition. As mentioned before, seasonal estimates of these variables (e.g. *HOF*) would enhance our understanding of the relation between them and the LM parameters.

Even though the model to predict b (Equations (3)–(5)) is weaker ($R^2 = 0.25$–0.47) than the model to predict m ($R^2 = 0.54$, Equation (2)), the sensitivity of the t_a–t_s fit to deviations in m is more significant than to deviations in b. Figure 8 presents the mean variation in the Nash–Sutcliffe (NS) coefficient (Nash and Sutcliffe, 1970) and mean standard error with deviations in m and b between 0% and 25% and 0 and 1.6 °C, respectively. These ranges of deviation included 85% of the distributions of the difference between observed and predicted m and b depicted in panel b (Figures 6 and 7).

Model validation and application

The performance of the model in predicting stream water temperature greater than 0 °C was evaluated with the NS coefficient and the R^2. The ability of the LM to predict the stream water temperature time series at each site on the basis of their local t_a–t_s relationship yielded a mean value of 0.94. In contrast, the mean NS attained by computing the LM parameters (m and b), using the regional model (Equations (2)–(5)) yielded a mean NS of 0.79 (Figure 9). The mean difference between these NS values is 0.15. Even though the NS values for the modelled time series of stream temperature were lower than those on the basis of site-specific observations, 80% of all sites reported a modelled NS greater than 0.8. The difference between NS of observed and modelled stream temperatures is greater than 25% at 16 sites located across CA (three sites), OR (two sites), WA (three sites), WI (three sites), CO (one site), NC (two sites), FL (one site) and NV (one site, Figure 10). Thirteen of these sites have a difference between observed and predicted slope >25%. However, at seven sites, the predicted NS is greater than 0.5. In the majority of these sites (10 out of 13), the slope

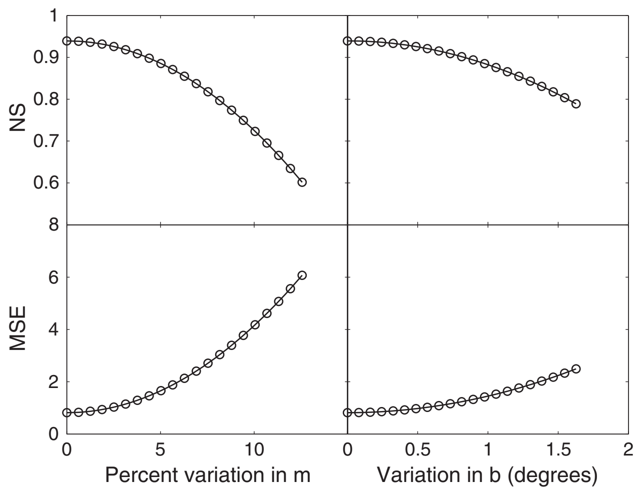

Figure 8. Mean sensitivity of the t_a–t_s fit in terms of Nash–Sutcliffe (NS) coefficient and mean square error (MSE) to changes in slope (m) and intercept (b)

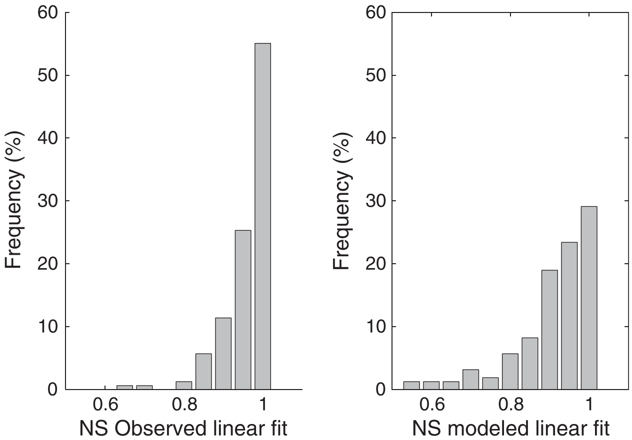

Figure 9. Histograms of observed and predicted Nash–Sutcliffe (NS) coefficients of the fits of stream temperature (t_s). The left panel presents the observed NS attained considering the linear site relations (i.e. local m and b). The right panel presents the modelled NS archived using the multiple linear regression model (Equations (2)–(5))

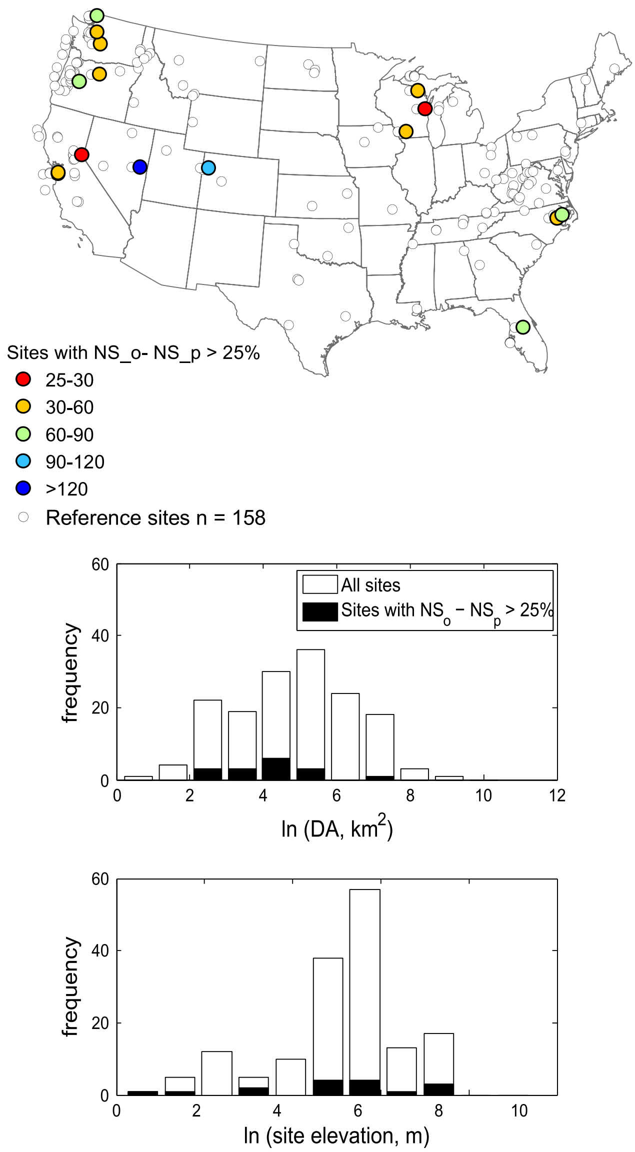

Figure 10. Sites for which the difference between observed (NS_o) and predicted (NS_p) Nash–Sutcliffe is greater than 25%

of the linear t_a–t_s relation is over predicted. No spatial pattern was depicted for these sites. However, the sites tend to be located in western states and have relatively low *DA* (26–1525 km^2, Figure 10).

For independent validation, the model described by Equations (2)–(5) was applied to compute the slope and intercept (with $t_a > 0\,°C$) at 89 nonreference sites (Figure 2) across the USA, on the basis solely of basin characteristics (*DA*, *P*, *T*, *BF*, Q, *HOF*, *C*, *F*, *F1*, *U1* and *H*). These predicted values of m and b were then used to compute the t_s time series. The comparison between observations and the predictions yielded a mean NS of 0.46, with 61% of the sites having NS > 0.7. This indicated that the model derived for reference sites can also be used for nonreference sites. This application provided an approximation of the relation between air and stream water temperature anywhere in the CONUS where stream temperature data are not available.

Even though the model developed in this study has large uncertainties, particularly with respect to the intercept, we believe it provides a coarse planning tool that could eventually be used to model climate change impacts in rivers and streams across the USA. The underlying assumption in doing so would be that the historic relation between air and stream temperature holds in the future. We used this assumption of time persistence relation between t_s and t_a to investigate climate change impacts in t_s in 61 streams of the southeast region of the USA and found that most sites experienced increases in historic (1961–2010) mean annual t_s of 0.1 °C per decade, although all sites were projected to experience increases in future (2011–2060) t_s of 0.41 °C per decade (Caldwell *et al.*, 2014). The aforementioned assumption of static behaviour is analogous to the assumptions made to derive some of the most widely used bias corrected climate projections (Wood *et al.*, 2004; Meehl *et al.*, 2007). In fact, such bias corrected projections have been recently used as climatic inputs of complex process-based models to predict t_s temperature (Wu *et al.*, 2012; Ficklin *et al.*, 2013; van Vliet *et al.*, 2013).

Seasonal thermal sensitivity (m)

Thermal sensitivity has been defined as the slope (m) of the stream–air temperature relationship (Kelleher *et al.*, 2012; Mayer, 2012). We analysed the temporal pattern of thermal sensitivity on the basis of weekly data by computing m (i.e. slope of the linear relation between t_a

and t_s) for three seasons (spring, summer and fall) independently. This analysis also provided information regarding hysteresis in the t_a–t_s relationship. The seasonal linear relations between t_s and t_a yielded a mean R^2 between 0.67 and 0.92 (Figure 11). These fits included sites with at least 40 weekly observations per season excluding t_a values less than 0 °C. The model fits were stronger for fall ($R^2 = 0.92 \pm 0.04$) and weaker for summer ($R^2 = 0.67 \pm 0.15$; Figure 11). Examples of the seasonal linear fits for the five sites are presented in Figure 12. We found that the mean thermal sensitivity varied between 0.63 ± 0.22 and 0.74 ± 0.22 across all seasons (Figure 11). Thermal sensitivity for the spring season was significantly lower than for the other two seasons (Tukey Kramer HSD, $p = 0.002$–0.02, Figure 11). Lower thermal sensitivities have been observed for the summer compared with annual time series in the Pacific Northwest (Mayer, 2012). However, a direct comparison with the results by Mayer (2012) is not possible because he did not analyse any other seasons. This difference in the slope of the relationship between t_a and t_s for different seasons illustrates the hysteresis that has been reported before (Mohseni *et al*., 1998; Mantua *et al*., 2010). Thermal sensitivity (m) is significantly lower ($p < 0.05$) for the spring than for the fall in 73% of the sites.

Six out of the 17 dependent variables considered in this study (Table III) were found to be significant predictors of the seasonal thermal sensitivity, m (Table V). Multiple regression models (not shown here for brevity) yield R^2 values between 0.17 and 0.60 (Table V). As for the case of the model derived to predict monthly thermal sensitivity (Equation (2)), we found that *DA* explained a significant proportion (3–17%) of the variability in thermal sensitivity for all seasons. The cooling effect of groundwater (i.e. *BF*) on thermal sensitivity was only evident for the spring and fall seasons, explaining 5% and 21% of the variance, respectively. Even though the cooling effect of groundwater was not evident in the summer thermal sensitivity, we found that it explained a significant proportion of the variance in mean summer t_s (refer to the succeeding texts). Mean basin slope (S) explains 54% of the variance for the spring season m. This relationship is likely related to the shorter residence time of water in steep catchments (refer to the succeeding texts). Other variables (H, P and Q) were also significantly correlated but explained less than 5% of the terminal sensitivity variance (Table V).

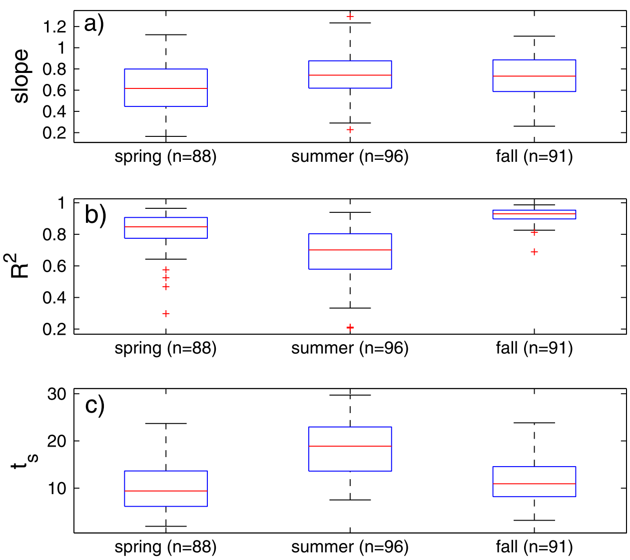

Figure 11. Distribution of the slope and R^2 for the linear fits between t_a and t_s for three seasons at all reference sites (panels a and b). Panel c presents the distributions of the mean stream temperature (t_s) for each of the three seasons considered

Mean seasonal stream water temperature (t_s) varied between 10.3 ± 4.9 °C for spring and 18.6 ± 5.5 °C for summer (Figure 11). We used multiple regression to investigate the effect of air temperature (T), groundwater (*BF*), discharge (Q), precipitation (P), drainage area (*DA*), topographic setting (S and H) and forest cover (F and $F1$) on seasonal mean t_s. We did not include all 17 variables available in Table III because our objective here was to find mechanistic relations rather than to predict the mean seasonal t_s. We found very strong R^2 values (0.85–0.92) for the three seasonal multivariate models (Table V). These models included all of the variables considered except for P. In all three models, the atmospheric conditions (T) and topographic setting (S) explained a large portion of the variance (5–78%). Not surprisingly, T was a strong predictor of t_a explaining between 22% and 78% of its variance. This relationship has been long established (Stefan and Preudhomme, 1993; Webb and Nobilis, 1997; Caissie *et al*., 1998; Donato, 2002; Ducharne, 2008; Webb *et al*., 2008). Thus, we decided to investigate separately the effects of the other potential controllers and found slightly weaker models ($R^2 = 0.63$–0.82) for which six variables explained most of the t_s variance: S, *BF*, H, Q, *DA* and P. The first four are inversely related to t_s, whereas *DA* and P are positively related. Other studies have found the strong predicting power of S, H and *DA* on mean annual t_s (Donato, 2002) and of *BF* on mean August temperatures (Mayer, 2012). An interpretation for the negative correlation between t_s and S and H is because surface water in steeper sub basins, typically located at higher elevations (H and S are correlated, $R^2 = 0.18$, $p < 0.0001$), have shorter residence time to gain heat from their surroundings and, thus, tend to stay cooler (Donato, 2002). This would particularly be the case for the mean summer temperatures for which slope explained 54% of the variance (Table V). Other studies

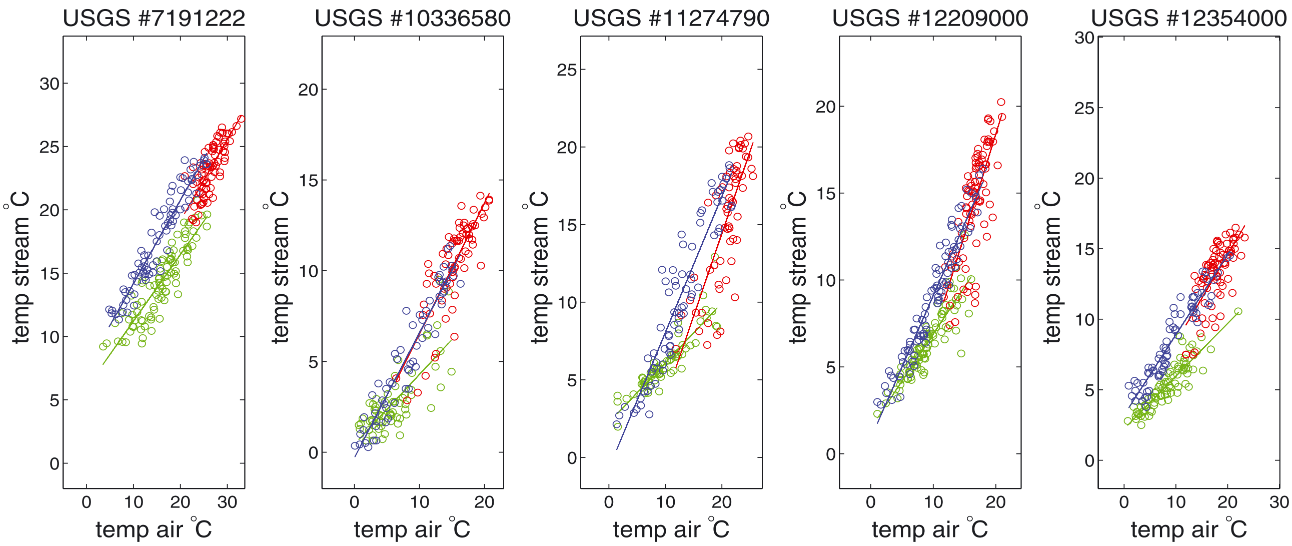

Figure 12. Examples of the linear model (LM) fitted to seasonal 7-day mean values of air (t_a) and stream (t_s) at five U.S. Geological Survey (USGS) sites: #07191222 (Beaty Creek near Jay, OK), #10336580 (Upper Truckee Rv at S Upper Truckee Rd near Meyers, CA), #11274790 (Tuolumne R A Grand Canyon of Tuolumne Ab Hetch Hetchy, CA), #12209000 (SF Nooksack River near Wickersham, WA) and # 12354000 (St Regis River near St Regis, MT). Green, red and blue markers are spring, summer and fall, respectively

have documented the cooling effect of groundwater on mean stream temperature (i.e. *BF* inversely related to t_s). A study over a 266 km river reach in France found a significant cooling effect of groundwater during August (Moatar and Gailhard, 2006). Another study found that groundwater explained the summer stream temperature variations in two small British Columbia catchments (Story *et al.*, 2003). Like others, we found that larger catchments tend to have higher t_s (Donato, 2002; Mayer, 2012). Finally, the increasing heat capacity and travel times in basins with higher flows could explain the negative correlation between Q and t_s (Webb *et al.*, 2008). Mean annual precipitation (P) is positively related to mean t_s in the spring and fall seasons but explains less than 1.5% of the variance.

CONCLUSIONS

We developed an empirical model to predict stream water temperature across the CONUS on the basis of air temperature and basin characteristics. Multiple linear regression models were formulated to predict the slope (m) and intercept (b) of the linear relationship between air and stream water temperature for air temperatures greater than 0°. The predicting variables of m include drainage area, base flow index, precipitation, elevation and percent forest cover in the riparian area. The formulated equations to predict b were derived considering three altitudinal ranges for which the main predictors are drainage area, mean annual air temperature and discharge and basin and riparian forest cover percentages. We conclude that the model developed in this study can provide a robust approximation of historic time series of stream water temperature anywhere in the USA. In addition, the model can potentially be used to examine general patterns of stream water temperatures at a large scale under future climate scenarios.

Our seasonal thermal sensitivity analysis not only highlighted hysteresis in air–water temperature relationship (i.e. mean spring water temperature is lower than mean fall water temperature) but also the strong control that some watershed characteristics such as drainage area, topography, vegetation cover and hydrogeological settings have on both seasonal thermal sensitivity and mean seasonal stream temperatures. We conclude that specific watershed characteristics identified in this study must be considered in assessing the impacts of climate change on stream temperature across the USA. Therefore, watershed management strategies should be designed to fit local watershed conditions to be most effective to protect aquatic resources under a changing climate.

ACKNOWLEDGEMENTS

This study was funded by the National Science Foundation EaSM programme (AGS-1049200) at NCSU and the Eastern Forest Environment Threat Assessment Center (EFETAC), USDA Forest Service.

REFERENCES

Allen D, Dietrich WE, Baker PF, Ligon F, Orr B. 2007. Development of a mechanistically based, basin-scale stream temperature model: applications to cumulative effects modeling. In *Proceedings of the Redwood*

Region Forest Science Symposium: What Does the Future Hold?, Standiford RB (ed.) Forest Service, USDA: Albany, CA; 11–24.

Arismendi I, Johnson SL, Dunham JB, Haggerty R, Hockman-Wert D. 2012. The paradox of cooling streams in a warming world: regional climate trends do not parallel variable local trends in stream temperature in the Pacific continental United States. *Geophysical Research Letters* **39**: L10401–L10401. DOI: 10.1029/2012GL051448.

Beitinger TL, Bennett WA, McCauley RW. 2000. Temperature tolerances of North American freshwater fishes exposed to dynamic changes in temperature. *Environmental Biology of Fishes* **58**: 237–275. DOI: 10.1023/A:1007676325825.

Beschta RL. 1997. Riparian shade and stream temperature: an alternative perspective. *Rangelands* **19**: 25–28.

Beschta RL, Weatherred J. 1984. TEMP-84: a computer model for predicting stream temperatures resulting from the management of streamside vegetation USDA forest service watershed system development group.

Bicknell BR. 1997. Hydrological Simulation Program–FORTRAN (HSPF: user's manual for release 11). EPA-600/R-97/0/80.

Bogan T, Mohseni O, Stefan HG. 2003. Stream temperature-equilibrium temperature relationship. *Water Resources Research* **39**: 1245–1245. DOI: 10.1029/2003WR002034.

Booth DB, Kraseski KA, Jackson CR. 2014. Local-scale and watershed-scale determinants of summertime urban stream temperatures. *Hydrological Processes* **28**: 2427–2438. DOI: 10.1002/hyp.9810.

Boyd M, Kasper B. 2003. Analytical methods for dynamic open channel heat and mass transfer: methodology for heat source model version 7.0.

Brown GW. 1969. Predicting temperatures of small streams. *Water Resources Research* **5**: 68-&. DOI: 10.1029/WR005i001p00068.

Brown GW, Krygier JT. 1970. Effects of clear-cutting on stream temperature. *Water Resources Research* **6**: 1133-&. DOI: 10.1029/WR006i004p01133.

Bustillo V, Moatar F, Ducharne A, Thiery D, Poirel A. 2014. A multimodel comparison for assessing water temperatures under changing climate conditions via the equilibrium temperature concept: case study of the Middle Loire River, France. *Hydrological Processes* **28**: 1507–1524. DOI: 10.1002/hyp.9683.

Caissie D. 2006. The thermal regime of rivers: a review. *Freshwater Biology* **51**: 1389–1406. DOI: 10.1111/j.1365-2427.2006.01597.x.

Caissie D, El-Jabi N, St-Hilaire A. 1998. Stochastic modelling of water temperatures in a small stream using air to water relations. *Canadian Journal of Civil Engineering* **25**: 250–260. DOI: 10.1139/cjce-25-2-250.

Caldwell P, Segura C, Gull Laird S, Ge S, McNulty SG, Sandercock M, Boggs J, Vose JM. 2014. Short-term stream water temperature observations permit rapid assessment of potential climate change impacts. *Hydrological Processes*.

Chen YD, Carsel RF, McCutcheon SC, Nutter WL. 1998. Stream temperature simulation of forested riparian areas: I. Watershed-scale model development. *Journal of Environmental Engineering-Asce* **124**: 304–315. DOI: 10.1061/(ASCE)0733-9372(1998)124:4(304).

Crisp DT, Howson G. 1982. Effect of air-temperature upon mean water temperature in streams in the north Pennines and English Lake District. *Freshwater Biology* **12**: 359–367. DOI: 10.1111/j.1365-2427.1982.tb00629.x.

Danehy RJ, Colson CG, Parrett KB, Duke SD. 2005. Patterns and sources of thermal heterogeneity in small mountain streams within a forested setting. *Forest Ecology and Management* **208**: 287–302. DOI: 10.1016/j.foreco.2004.12.006.

Donato MM. 2002. A statistical model for estimating stream temperatures in the salmon and clearwater river basins, Central Idaho. In: Water-Resources Investigations Report 02–4195, USGS (ed.).

Ducharne A. 2008. Importance of stream temperature to climate change impact on water quality. *Hydrology and Earth System Sciences* **12**: 797–810.

Eaton JG, Scheller RM. 1996. Effects of climate warming on fish thermal habitat in streams of the United States. *Limnology and Oceanography* **41**: 1109–1115.

Ebersole JL, Liss WJ, Frissell CA. 2001. Relationship between stream temperature, thermal refugia and rainbow trout *Oncorhynchus mykiss* abundance in arid-land streams in the northwestern United States. *Ecology of Freshwater Fish* **10**: 1–10. DOI: 10.1034/j.1600-0633.2001.100101.x.

Edinger JE, Duttweil D, Geyer JC. 1968. Response of water temperatures to meteorological conditions. *Water Resources Research* **4**: 1137-&. DOI: 10.1029/WR004i005p01137.

Erickson TR, Stefan HG. 1996. Correlations of Oklahoma stream temperatures with air temperatures.

Erickson TR, Stefan HG. 2000. Linear air/water temperature correlations for streams during open water periods. *Journal of Hydrologic Engineering* **5**: 317–321. DOI: 10.1061/(ASCE)1084-0699(2000)5:3(317).

Evans EC, Petts GE. 1997. Hyporheic temperature patterns within riffles. *Hydrological Sciences Journal-Journal Des Sciences Hydrologiques* **42**: 199–213. DOI: 10.1080/02626669709492020.

Falcone JA. 2011. Geospatial attributes of gages for evaluating streamflow. Digital spatial data set. URL: http://water.usgs.gov/GIS/metadata/usgswrd/XML/gagesII_Sept2011.xml.

Falcone JA, Carlisle DM, Wolock DM, Meador MR. 2010. GAGES: a stream gage database for evaluating natural and altered flow conditions in the conterminous united states. *Ecology* **91**: 621. DOI: 10.1890/09.1.

Ficke AD, Myrick CA, Hansen LJ. 2007. Potential impacts of global climate change on freshwater fisheries. *Reviews in Fish Biology and Fisheries* **17**: 581–613. DOI: 10.1007/s11160-007-9059-5.

Ficklin DL, Luo Y, Stewart IT, Maurer EP. 2012. Development and application of a hydroclimatological stream temperature model within the Soil and Water Assessment Tool. *Water Resources Research* **48**: W01511–W01511. DOI: 10.1029/2011WR011256.

Ficklin DL, Stewart IT, Maurer EP. 2013. Effects of climate change on stream temperature, dissolved oxygen, and sediment concentration in the Sierra Nevada in California. *Water Resources Research* **49**: 2765–2782. DOI: 10.1002/wrcr.20248.

Furey PR, Gupta VK. 2005. Effects of excess rainfall on the temporal variability of observed peak-discharge power laws. *Advances in Water Resources* **28**: 1240–1253. DOI: 10.1016/j.advwatres.2005.03.014.

Gu RC, Montgomery S, Al AT. 1998. Quantifying the effects of stream discharge on summer river temperature. *Hydrological Sciences Journal-Journal Des Sciences Hydrologiques* **43**: 885–904. DOI: 10.1080/02626669809492185.

Gupta VK, Mesa OJ, Dawdy DR. 1994. Multiscaling theory of flood peaks – regional quantile analysis. *Water Resources Research* **30**: 3405–3421. DOI: 10.1029/94wr01791.

Haag I, Luce A. 2008. The integrated water balance and water temperature model LARSIM-WT. *Hydrological Processes* **22**: 1046–1056. DOI: 10.1002/hyp.6983.

Hari RE, Livingstone DM, Siber R, Burkhardt-Holm P, Guttinger H. 2006. Consequences of climatic change for water temperature and brown trout populations in Alpine rivers and streams. *Global Change Biology* **12**: 10–26. DOI: 10.1111/j.1365-2486.2005.01051.x.

Hawkins CP, Hogue JN, Decker LM, Feminella JW. 1997. Channel morphology, water temperature, and assemblage structure of stream insects. *Journal of the North American Benthological Society* **16**: 728–749. DOI: 10.2307/1468167.

Isaak DJ, Wollrab S, Horan D, Chandler G. 2012. Climate change effects on stream and river temperatures across the northwest US from 1980-2009 and implications for salmonid fishes. *Climatic Change* **113**: 499–524. DOI: 10.1007/s10584-011-0326-z.

Johnson SL. 2004. Factors influencing stream temperatures in small streams: substrate effects and a shading experiment. *Canadian Journal of Fisheries and Aquatic Sciences* **61**: 913–923. DOI: 10.1139/F04-040.

Kaushal SS, Likens GE, Jaworski NA, Pace ML, Sides AM, Seekell D, Belt KT, Secor DH, Wingate RL. 2010. Rising stream and river temperatures in the United States. *Frontiers in Ecology and the Environment* **8**: 461–466. DOI: 10.1890/090037.

Kelleher C, Wagener T, Gooseff M, McGlynn B, McGuire K, Marshall L. 2012. Investigating controls on the thermal sensitivity of Pennsylvania streams. *Hydrological Processes* **26**: 771–785. DOI: 10.1002/hyp.8186.

Kim KS, Chapra SC. 1997. Temperature model for highly transient shallow streams. *Journal of Hydraulic Engineering-Asce* **123**: 30–40. DOI: 10.1061/(ASCE)0733-9429(1997)123:1(30).

Langan SJ, Johnston L, Donaghy MJ, Youngson AF, Hay DW, Soulsby C. 2001. Variation in river water temperatures in an upland stream over a 30-year period. *Science of the Total Environment* **265**: 195–207. DOI: 10.1016/S0048-9697(00)00659-8.

LeBlanc RT, Brown RD, FitzGibbon JE. 1997. Modeling the effects of land use change on the water temperature in unregulated urban streams. *Journal of Environmental Management* **49**: 445–469. DOI: 10.1006/jema.1996.0106.

Loinaz MC, Davidsen HK, Butts M, Bauer-Gottwein P. 2013. Integrated flow and temperature modeling at the catchment scale. *Journal of Hydrology* **495**: 238–251. DOI: 10.1016/j.hydrol.2013.04.039.

Mantua N, Tohver I, Hamlet A. 2010. Climate change impacts on streamflow extremes and summertime stream temperature and their possible consequences for freshwater salmon habitat in Washington State. *Climatic Change* **102**: 187–223. DOI: 10.1007/s10584-010-9845-2.

Marquard DW. 1970. Generalized inverses, ridge regression, biased linear estimation, and nonlinear estimation. *Technometrics* **12**: 591-&. DOI: 10.2307/1267205.

MATLAB. 2010. Version 7.10.0 (R2010a). The MathWorks Inc.

Mayer TD. 2012. Controls of summer stream temperature in the Pacific Northwest. *Journal of Hydrology* **475**: 323–335. DOI: 10.1016/j.jhydrol.2012.10.012.

Meehl GA, Covey C, Delworth T, Latif M, McAvaney B, Mitchell JFB, Stouffer RJ, Taylor KE. 2007. The WCRP CMIP3 multi-model dataset: a new era in climate change research. *Bulletin of the American Meteorological Society* **88**: 1383–1394.

Meier W, Bonjour C, Wuest A, Reichert P. 2003. Modeling the effect of water diversion on the temperature of mountain streams. *Journal of Environmental Engineering-Asce* **129**: 755–764. DOI: 10.1061/(ASCE)0733-9372(2003)129:8(755).

Moatar F, Gailhard J. 2006. Water temperature behaviour in the River Loire since 1976 and 1881. *Comptes Rendus Geoscience* **338**: 319–328. DOI: 10.1016/j.crte.2006.02.011.

Mohseni O, Erickson TR, Stefan HG. 1999. Sensitivity of stream temperatures in the United States to air temperatures projected under a global warming scenario. *Water Resources Research* **35**: 3723–3733. DOI: 10.1029/1999WR900193.

Mohseni O, Stefan HG. 1999. Stream temperature air temperature relationship: a physical interpretation. *Journal of Hydrology* **218**: 128–141. DOI: 10.1016/S0022-1694(99)00034-7.

Mohseni O, Stefan HG, Erickson TR. 1998. A nonlinear regression model for weekly stream temperatures. *Water Resources Research* **34**: 2685–2692. DOI: 10.1029/98WR01877.

Mohseni O, Stefan HG, Eaton JG. 2003. Global warming and potential changes in fish habitat in US streams. *Climatic Change* **59**(3): 389–409.

Moore RD, Spittlehouse DL, Story A. 2005. Riparian microclimate and stream temperature response to forest harvesting: a review. *Journal of the American Water Resources Association* **41**: 813–834.

Morrill JC, Bales RC, Conklin MH. 2005. Estimating stream temperature from air temperature: implications for future water quality. *Journal of Environmental Engineering-Asce* **131**: 139–146. DOI: 10.1061/(ASCE)0733-9372(2005)131:1(139).

Nash JE, Sutcliffe JV. 1970. River flow forecasting through conceptual models I. A discussion of principles. *Journal of Hydrology* **10**: 282–290.

Nelson KC, Palmer MA. 2007. Stream temperature surges under urbanization and climate change: data, models, and responses. *Journal of the American Water Resources Association* **43**: 440–452. DOI: 10.1111/j.1752-1688.2007.00034.x.

Norton GE, Bradford A. 2009. Comparison of two stream temperature models and evaluation of potential management alternatives for the Speed River, Southern Ontario. *Journal of Environmental Management* **90**: 866–878. DOI: 10.1016/j.jenvman.2008.02.002.

O'Driscoll MA, DeWalle DR. 2006. Stream-air temperature relations to classify stream-ground water interactions. *Journal of Hydrology* **329**: 140–153. DOI: 10.1016/j.jhydrol.2006.02.010.

Olden JD, Naiman RJ. 2010. Incorporating thermal regimes into environmental flows assessments: modifying dam operations to restore freshwater ecosystem integrity. *Freshwater Biology* **55**: 86–107. DOI: 10.1111/j.1365-2427.2009.02179.x.

Ozaki N, Fukushima T, Harasawa H, Kojiri T, Kawashima K, Ono M. 2003. Statistical analyses on the effects of air temperature fluctuations on river water qualities. *Hydrological Processes* **17**: 2837–2853. DOI: 10.1002/hyp.1437.

Pilgrim JM, Fang X, Stefan HG. 1998. Stream temperature correlations with air temperatures in Minnesota: implications for climate warming. *Journal of the American Water Resources Association* **34**: 1109–1121. DOI: 10.1111/j.1752-1688.1998.tb04158.x.

Poff NL, Richter BD, Arthington AH, Bunn SE, Naiman RJ, Kendy E, Acreman M, Apse C, Bledsoe BP, Freeman MC, Henriksen J, Jacobson RB, Kennen JG, Merritt DM, O'Keeffe JH, Olden JD, Rogers K, Tharme RE, Warner A. 2010. The ecological limits of hydrologic alteration (ELOHA): a new framework for developing regional environmental flow standards. *Freshwater Biology* **55**: 147–170. DOI: 10.1111/j.1365-2427.2009.02204.x.

Poole GC, Berman CH. 2001. An ecological perspective on in-stream temperature: natural heat dynamics and mechanisms of human-caused thermal degradation. *Environmental Management* **27**: 787–802. DOI: 10.1007/s002670010188.

Richardson JS, Danehy RJ. 2007. A synthesis of the ecology of headwater streams and their riparian zones in temperate forests. *Forestry Sciences* **53**: 131–147.

Roman DC, Vogel RM, Schwarz GE. 2012. Regional regression models of watershed suspended-sediment discharge for the eastern United States. *Journal of Hydrology* **472**: 53–62. DOI: 10.1016/j.jhydrol.2012.09.011.

Roth TR, Westhoff MC, Huwald H, Huff JA, Rubin JF, Barrenetxea G, Vetterli M, Parriaux A, Selker JS, Parlange MB. 2010. Stream temperature response to three riparian vegetation scenarios by use of a distributed temperature validated model. *Environmental Science & Technology* **44**: 2072–2078. DOI: 10.1021/es902654f.

Sand-Jensen K, Pedersen NL. 2005. Differences in temperature, organic carbon and oxygen consumption among lowland streams. *Freshwater Biology* **50**: 1927–1937. DOI: 10.1111/j.1365-2427.2005.01436.x.

Segura C, James AL, Lazzati D, Roulet NT. 2012. Scaling relationships for event water contributions and transit times in small-forested catchments in Eastern Quebec. *Water Resources Research* **48**: W07502–W07502. DOI: 10.1029/2012WR011890.

Segura C, Lazzati D, Sankarasubramanian A. 2013. The use of broken power-laws to describe the distributions of daily flow above the mean annual flow across the conterminous US. *Journal of Hydrology* **505**: 35–46. DOI: 10.1016/j.jhydrol.2013.09.016.

Segura C, Pitlick J. 2010. Scaling frequency of channel-forming flows in snowmelt-dominated streams. *Water Resources Research* **46**: W06524–W06524, doi: 06510.01029/02009WR008336. DOI: 10.1029/2009WR008336.

Shapiro SS, Wilk MB. 1965. An analysis of variance test for normality (complete samples). *Biometrika* **52**: 591-&. DOI: 10.2307/2333709.

Sinokrot BA, Stefan HG. 1993. Stream temperature dynamics – measurements and modeling. *Water Resources Research* **29**: 2299–2312. DOI: 10.1029/93WR00540.

Stefan HG, Preudhomme EB. 1993. Stream temperature estimation from air-temperature. *Water Resources Bulletin* **29**: 27–45.

Stefan HG, Sinokrot BA. 1993. Projected global climate-change impact on water temperatures in 5 north central united-states streams. *Climatic Change* **24**: 353–381. DOI: 10.1007/BF01091855.

Story A, Moore RD, Macdonald JS. 2003. Stream temperatures in two shaded reaches below cutblocks and logging roads: downstream cooling linked to subsurface hydrology. *Canadian Journal of Forest Research-Revue Canadienne De Recherche Forestiere* **33**: 1383–1396. DOI: 10.1139/x03-087.

Studinski JM, Hartman KJ, Niles JM, Keyser P. 2012. The effects of riparian forest disturbance on stream temperature, sedimentation, and morphology. *Hydrobiologia* **686**: 107–117. DOI: 10.1007/s10750-012-1002-7.

Tague C, Farrell M, Grant G, Lewis S, Rey S. 2007. Hydrogeologic controls on summer stream temperatures in the McKenzie River basin, Oregon. *Hydrological Processes* **21**: 3288–3300. DOI: 10.1002/hyp.6538.

Thornton PE, Thornton MM, Mayer BW, Wilhelmi B, Wei Y, Cook RB. 2012. Daymet: daily surface weather on a 1 km grid for north america, 1980-2012.

van Vliet MTH, Ludwig F, Zwolsman JJG, Weedon GP, Kabat P. 2011. Global river temperatures and sensitivity to atmospheric warming and changes in river flow. *Water Resources Research* **47**: W02544.

van Vliet MTH, Franssen WHP, Yearsley JR, Ludwig F, Haddeland I, Lettenmaier DP, Kabat P. 2013. Global river discharge and water temperature under climate change. *Global Environmental Change* **23**: 450–464. DOI: 10.1016/j.gloenvcha.2012.11.002.

Vannote RL, Minshall GW, Cummins KW, Sedell JR, Cushing CE. 1980. River continuum concept. *Canadian Journal of Fisheries and Aquatic Sciences* **37**: 130–137.

Vogel RM, Sankarasubramanian A. 2000. Spatial scaling properties of annual streamflow in the United States. *Hydrological Sciences Journal-Journal Des Sciences Hydrologiques* **45**. DOI: 10.1080/02626660009492342.

Webb BW, Clack PD, Walling DE. 2003. Water–air temperature relationships in a Devon river system and the role of flow. *Hydrological Processes* **17**: 3069–3084. DOI: 10.1002/hyp.1280.

Webb BW, Hannah DM, Moore RD, Brown LE, Nobilis F. 2008. Recent advances in stream and river temperature research. *Hydrological Processes* **22**: 902–918. DOI: 10.1002/hyp.6994.

Webb BW, Nobilis F. 1994. Water temperature behavior in the river Danube during the 20th-century. *Hydrobiologia* **291**: 105–113. DOI: 10.1007/BF00044439.

Webb BW, Nobilis F. 1997. Long-term perspective on the nature of the air-water temperature relationship: a case study. *Hydrological Processes* **11**: 137–147. DOI: 10.1002/(SICI)1099-1085(199702)11:2<137::AID-HYP405>3.3.CO;2-U.

Webb BW, Nobilis F. 2007. Long-term changes in river temperature and the influence of climatic and hydrological factors. *Hydrological Sciences Journal-Journal Des Sciences Hydrologiques* **52**: 74–85. DOI: 10.1623/hysj.52.1.74.

Webb BW, Walling DE. 1993. Longer-term water temperature behavior in an upland stream. *Hydrological Processes* **7**: 19–32. DOI: 10.1002/hyp.3360070104.

Webb BW, Zhang Y. 1997. Spatial and seasonal variability in the components of the river heat budget. *Hydrological Processes* **11**: 79–101. DOI: 10.1002/(SICI)1099-1085(199701)11:1<79::AID-HYP404>3.3.CO;2-E.

Whitehead PG, Wilby RL, Battarbee RW, Kernan M, Wade AJ. 2009. A review of the potential impacts of climate change on surface water quality. *Hydrological Sciences Journal-Journal Des Sciences Hydrologiques* **54**: 101–123. DOI: 10.1623/hysj.54.1.101.

Wood AW, Leung LR, Sridhar V, Lettenmaier DP. 2004. Hydrologic implications of dynamical and statistical approaches to downscaling climate model outputs. *Climatic Change* **62**: 189–216. DOI: 10.1023/B:CLIM.0000013685.99609.9e.

Wu H, Kimball JS, Elsner MM, Mantua N, Adler RF, Stanford J. 2012. Projected climate change impacts on the hydrology and temperature of Pacific Northwest rivers. *Water Resources Research* **48**: W11530–W11530. DOI: 10.1029/2012WR012082.

Yearsley JR. 2009. A semi-Lagrangian water temperature model for advection-dominated river systems. *Water Resources Research* **45**: W12405–W12405. DOI: 10.1029/2008WR007629.

Younus M, Hondzo M, Engel BA. 2000. Stream temperature dynamics in upland agricultural watersheds. *Journal of Environmental Engineering-Asce* **126**: 518–526. DOI: 10.1061/(ASCE)0733-9372(2000)126:6(518).

